Indirect (source-free) integration method for EMRIs: waveforms from geodesic generic orbits and self-force consistent radial fall

Alessandro Spallicci[1]

Luca Bonetti[1], Stéphane Cordier[2], Richard Emilion[2], Sylvain Jubertie[3], Patxi Ritter[1,2]

Sofiane Aoudia

Université d'Orléans

[1] Observatoire des Sciences de l'Univers,
Laboratoire de Physique et Chimie de l'Environnement et de l'Espace,
LPC2E, UMR CNRS 7328, 3A Av. Recherche Scientifique, 45071 Orléans, France

[2] Laboratoire de Mathématiques, Analyse, Probabilités, Modèlisation,
MAPMO, UMR CNRS 7349, Rue de Chartres, 45067 Orléans, France

[3] Laboratoire d'Informatique Fondamentale,
LIFO, EA 4022, Rue de Leonardo da Vinci, 45067 Orléans, France

Capra XVII 2014

Plan of the talk

- Indirect (source-free) integration method for EMRIs: waveforms from geodesic generic orbits
- First order perturbation approach radial fall
- Self-force consistent radial fall

Johannes Droste

Physics. — "*On the field of a single centre in* EINSTEIN'*s theory of gravitation.*" By J. DROSTE. (Communicated by Prof. H. A. LORENTZ).

(Communicated in the meeting of December 30, 1914).

Droste J., 1915, Kon. Ned. Ak. Wet. Pr., 17, 998

Physics. — "*The field of a single centre in* EINSTEIN'S *theory of gravitation, and the motion of a particle in that field.*". By J. DROSTE. (Communicated by Prof. H. A. LORENTZ).

(Communicated in the meeting of May 27, 1916).

HET ZWAARTEKRACHTSVELD VAN EEN OF MEER LICHAMEN VOLGENS DE THEORIE VAN EINSTEIN.

PROEFSCHRIFT TER VERKRIJGING VAN DEN GRAAD VAN DOCTOR IN DE WIS- EN NATUURKUNDE AAN DE RIJKSUNIVERSITEIT TE LEIDEN, OP GEZAG VAN DEN RECTOR-MAGNIFICUS MR. C. VAN VOLLENHOVEN, HOOGLEERAAR IN DE FACULTEIT DER RECHTSGELEERDHEID, VOOR DE FACULTEIT DER WIS- EN NATUURKUNDE TE VERDEDIGEN OP VRIJDAG 8 DECEMBER 1916 TE 4 UREN DOOR **JOHANNES DROSTE**, GEBOREN TE GRAVE.

Droste J., 1917., Kon. Ned. Ak. Wet. Pr., 19, 197

$$ds^2 = \left(1 - \frac{\alpha}{r}\right) dt^2 - \frac{dr^2}{1 - \frac{\alpha}{r}} - r^2 (d\vartheta^2 + \sin^2 \vartheta \, d\rho^2)$$

Schwarzschild, January 1916

$$\boxed{R = (3x_1 + \rho)^{1/3} = (r^3 + \alpha^3)^{1/3}}$$

$$ds^2 = (1 - \alpha/R)dt^2 - \frac{dR^2}{1 - \alpha/R} - R^2 (d\vartheta^2 + \sin^2 \vartheta \, d\phi^2)$$

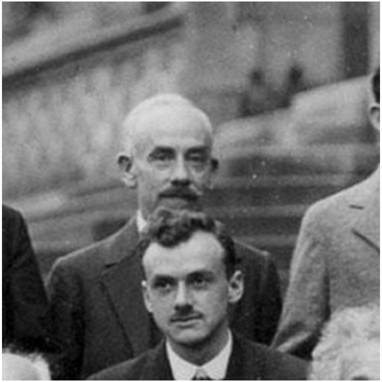

and FitzGerald...

Use of jump conditions

- Haas (PRD 2007)
- Field, Hesthaven, Lau (CQG 2009)
- Barack, Sago (PRD 2010)
- Cañizares, Sopuerta (PRD 2009); Cañizares, Sopuerta, Jaramillo (2010)
- Aoudia, Spallicci (PRD 2011), Ritter, Spallicci, Aoudia, Cordier (CQG 2011)

Indirect integration method: $h_{\mu\nu}$, Ψ in RW gauge

$$\frac{\partial^2\Psi^\ell(t,r)}{\partial r^{*2}} - \frac{\partial^2\Psi^\ell(t,r)}{\partial t^2} - V^\ell(r)\Psi^\ell(t,r) = S^\ell(t,r)\ , \tag{1}$$

$$S^\ell(t,r) = G^\ell(t,r)\delta[r-R(t)] + F^\ell(t,r)\delta'[r-R(t)]\ . \tag{2}$$

At the particle, we have $\Psi \in C^{-1}$

$h_{\mu\nu} \in C^0$ for radial infall, while it is more discontinuous for generic orbits. Jump conditions are derived either by

- the RWZ equation directly or by
- the inverse relations.

Once that the jump conditions are derived, we proceed as follows.

Indirect integration method: features

- Integration domain h discretised by 2-dimensional uniform mesh $(t,\ r_*)$.
- Initial data, empty cells, dealt as Lousto and Price, Martel and Poisson, Martel, Lousto, Haas.
- The forward time value at the upper node of the (r^*, t) grid cell is obtained by
  i) the preceding node values of the same cell,
  ii) analytic expressions from the jump conditions on Ψ and its derivatives,
  iii) AT HIGH ORDERS: the values of the wave function at adjacent cells .
- The numerical integration does not deal with the source and potential terms directly, for cells crossed by the particle world line.

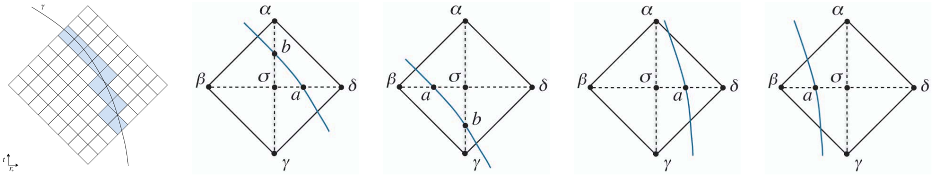

Case 1: particle crosses the β - δ line at a and γ - α line at b
$\epsilon_a = \min\{a\delta, a\beta\}$, $\epsilon_b = \min\{b\alpha, b\gamma\}$; $\Psi^\pm_b = \Psi^\pm(t_b, r^*_b)$, $\Psi^\pm_a = \Psi^\pm(t_a, r^*_a)$
6 analytic expressions and 6 numerical equations:

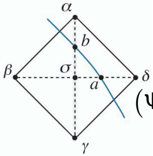

$$\left(\Psi^+ - \Psi^-\right)_a = [\Psi]_a \quad \left(\Psi^+_{,r^*} - \Psi^-_{,r^*}\right)_a = [\Psi_{,r^*}]_a \quad \left(\Psi^+_{,t} - \Psi^-_{,t}\right)_a = [\Psi_{,r^*}]_a \quad (3)$$

$$\left(\Psi^+ - \Psi^-\right)_b = [\Psi]_b \quad \left(\Psi^+_{,r^*} - \Psi^-_{,r^*}\right)_b = [\Psi_{,r^*}]_b \quad \left(\Psi^+_{,t} - \Psi^-_{,t}\right)_b = [\Psi_{,t}]_b \quad (4)$$

$$\Psi^+_\alpha = \Psi^+(t_b + \epsilon_b, r^*_b) = \Psi^+_b + \epsilon_b \, \Psi^+_{,t}\Big|_b \qquad (5)$$

$$\Psi^-_\sigma = \Psi^-(t_b - (h - \epsilon_b), r^*_b) = \Psi^-_b - (h - \epsilon_b) \, \Psi^-_{,t}\Big|_b \qquad (6)$$

$$\Psi^-_\gamma = \Psi^-(t_b - 2h + \epsilon_b, r^*_b) = \Psi^-(t_\sigma - h, r^*_b) = \Psi^-_\sigma - h \, \Psi^-_{,t}\Big|_\sigma \qquad (7)$$

$$\Psi^+_\delta = \Psi^+(t_a, r^*_a + \epsilon_a) = \Psi^+_a + \epsilon_a \, \Psi^+_{,r^*}\Big|_a \qquad (8)$$

$$\Psi^-_\sigma = \Psi^-(t_a, r^*_a - (h - \epsilon_a)) = \Psi^-_a - (h - \epsilon_a) \, \Psi^-_{,r^*}\Big|_a \qquad (9)$$

Our aim: determination of the value of Ψ^+_α, knowing those of Ψ^-_β, Ψ^-_γ, Ψ^+_δ, ϵ_a, ϵ_b, $[\Psi]_{a,b}$, $[\Psi_{,r}]_{a,b}$ and $[\Psi_{,t}]_{a,b}$
Through algebraic manipulation, we get

$$\Psi^+_\alpha = \Psi^-_\sigma + [\Psi]_b + [\Psi_{,t}]_b + h\ \Psi^-_{,t}\Big|_b \tag{11}$$

$$\Psi^+_\delta = \Psi^-_\sigma + [\Psi]_a + [\Psi_{,r^*}]_a + h\ \Psi^-_{,r^*}\Big|_a \tag{12}$$

$$\Psi^+_\alpha = \Psi^-_\beta - \Psi^-_\gamma + \Psi^+_\delta - [\Psi]_a + [\Psi]_b - \epsilon_a [\Psi_{,r^*}]_a + \epsilon_b [\Psi_{,t}]_b + \mathcal{O}(h^2) \tag{13}$$

- No need of direct integration of the singular source
- Top cell value depending upon analytic expressions (and other cell's corners)

Indirect integration method: second order for generic orbits

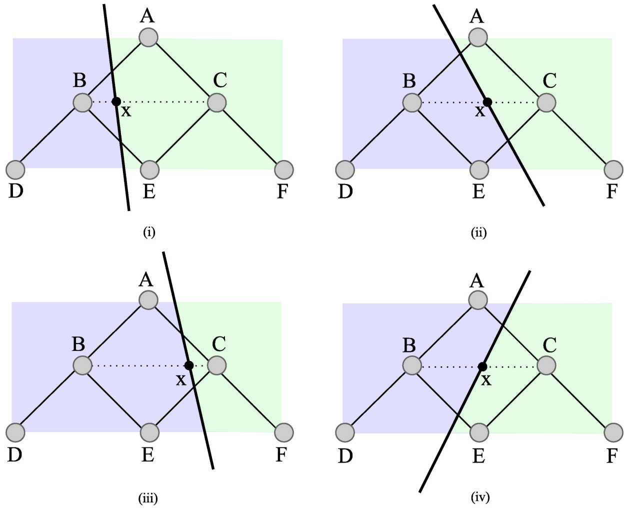

Figure: Second order mesh for the cells crossed by the particle. The number of grid nodes are six, for four cases.

Indirect method of integration: geodesic waveforms

Full agreement with previous results of other groups using other methods.

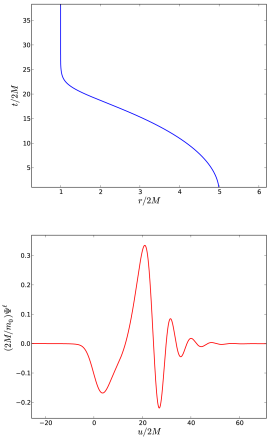

Radial fall from $r_0 = 5(2M)$ for the mode $\ell = 2$.

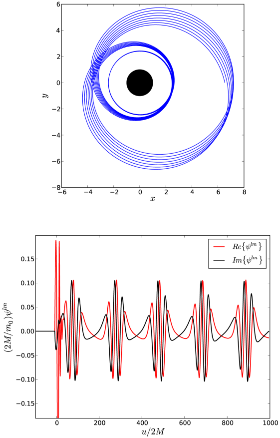

Odd parity waveform for an eccentric orbit $(e, p) = (0.5, 7.2)$ for the mode $(\ell, m) = (2, 1)$.

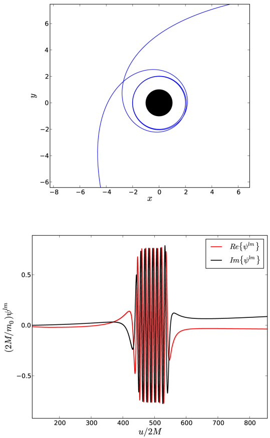

Even parity zoom-whirl waveform orbit $(e, p) = (1.0, 8.001)$ for the mode $(\ell, m) = (2, 2)$.

Geodesic waveforms (2nd order): circular ($\dot{E}^\infty_{\ell m}$)

ℓ	m	$\dot{E}^\infty_{\ell m}$	$\dot{E}^\infty_{\ell m}$ Poisson (1995,1997)	$\dot{E}^\infty_{\ell m}$ Martel 2004	$\dot{E}^\infty_{\ell m}$ Barack Lousto 2005	$\dot{E}^\infty_{\ell m}$ Sopuerta Laguna 2006
2	1	$8.1680.10^{-07}$	$8.1633.10^{-07}$ [0.06%]	$8.1623.10^{-07}$ [0.07%]	$8.1654.10^{-07}$ [0.03%]	$8.1662.10^{-07}$ [0.02%]
2	2	$1.7064.10^{-04}$	$1.7063.10^{-04}$ [0.006%]	$1.7051.10^{-04}$ [0.07%]	$1.7061.10^{-04}$ [0.02%]	$1.7064.10^{-04}$ [<0.001%]
3	1	$2.1757.10^{-09}$	$2.1731.10^{-09}$ [0.1%]	$2.1741.10^{-09}$ [0.07%]	$2.1734.10^{-09}$ [0.1%]	$2.1732.10^{-09}$ [0.1%]
3	2	$2.5203.10^{-07}$	$2.5199.10^{-07}$ [0.02%]	$2.5164.10^{-07}$ [0.2%]	$2.5207.10^{-07}$ [0.01%]	$2.5204.10^{-07}$ [0.002%]
3	3	$2.5471.10^{-05}$	$2.5471.10^{-05}$ [0.001%]	$2.5432.10^{-05}$ [0.2%]	$2.5479.10^{-05}$ [0.03%]	$2.5475.10^{-05}$ [0.02%]
4	1	$8.4124.10^{-13}$	$8.3956.10^{-13}$ [0.2%]	$8.3507.10^{-13}$ [0.7%]	$8.3982.10^{-13}$ [0.2%]	$8.4055.10^{-13}$ [0.08%]
4	2	$2.5099.10^{-09}$	$2.5091.10^{-09}$ [0.03%]	$2.4986.10^{-09}$ [0.5%]	$2.5099.10^{-09}$ [0.002%]	$2.5099.10^{-09}$ [0.002%]
4	3	$5.7750.10^{-08}$	$5.7751.10^{-08}$ [0.001%]	$5.7464.10^{-08}$ [0.5%]	$5.7759.10^{-08}$ [0.02%]	$5.7765.10^{-08}$ [0.03%]
4	4	$4.7251.10^{-06}$	$4.7256.10^{-06}$ [0.01%]	$4.7080.10^{-06}$ [0.4%]	$4.7284.10^{-06}$ [0.07%]	$4.7270.10^{-06}$ [0.04%]
5	1	$1.2632.10^{-15}$	$1.2594.10^{-15}$ [0.3%]	$1.2544.10^{-15}$ [0.7%]	$1.2598.10^{-15}$ [0.3%]	$1.2607.10^{-15}$ [0.2%]
5	2	$2.7910.10^{-12}$	$2.7896.10^{-12}$ [0.05%]	$2.7587.10^{-12}$ [1.2%]	$2.7877.10^{-12}$ [0.1%]	$2.7909.10^{-12}$ [0.003%]
5	3	$1.0933.10^{-09}$	$1.0933.10^{-09}$ [<0.001%]	$1.0830.10^{-09}$ [0.9%]	$1.0934.10^{-09}$ [0.009%]	$1.0936.10^{-09}$ [0.03%]
5	4	$1.2322.10^{-08}$	$1.2324.10^{-08}$ [0.01%]	$1.2193.10^{-08}$ [1.1%]	$1.2319.10^{-08}$ [0.03%]	$1.2329.10^{-08}$ [0.05%]
5	5	$9.4544.10^{-07}$	$9.4563.10^{-07}$ [0.02%]	$9.3835.10^{-07}$ [0.8%]	$9.4623.10^{-07}$ [0.08%]	$9.4616.10^{-07}$ [0.08%]
Total		$2.0293.10^{-04}$	$2.0292.10^{-04}$ [0.005%]	$2.0273.10^{-04}$ [0.096%]	$2.0291.10^{-04}$ [0.009%]	$2.0293.10^{-04}$ [<0.001%]

Table: Circular orbit: energy flux $\dot{E}_{\ell m}$ values at infinity, for different ℓm modes and $\ell < 5$ (units of M^2/m_0^2). The semi-latus rectum is $p = 7.9456$. The first column lists our results, and the second those of Poisson (1995,1997), the third of Martel (2004), the fourth of Barack and Lousto (2005), the fifth of Sopuerta and Laguna (2006).

ℓ	m	$\dot{L}^{\infty}_{\ell m}$	$\dot{L}^{\infty}_{\ell m}$ Poisson (1995,1997)	$\dot{L}^{\infty}_{\ell m}$ Martel (2004)	$\dot{L}^{\infty}_{\ell m}$ Sopuerta Laguna
2	1	$1.8294.10^{-05}$	$1.8283.10^{-05}$ [0.06%]	$1.8270.10^{-05}$ [0.1%]	$1.8289.10^{-05}$ [0.03%]
2	2	$3.8218.10^{-03}$	$3.8215.10^{-03}$ [0.009%]	$3.8164.10^{-03}$ [0.1%]	$3.8219.10^{-03}$ [0.002%]
3	1	$4.8729.10^{-08}$	$4.8670.10^{-08}$ [0.1%]	$4.8684.10^{-08}$ [0.09%]	$4.8675.10^{-08}$ [0.1%]
3	2	$5.6448.10^{-06}$	$5.6439.10^{-06}$ [0.02%]	$5.6262.10^{-06}$ [0.3%]	$5.6450.10^{-06}$ [0.003%]
3	3	$5.7048.10^{-04}$	$5.7048.10^{-04}$ [< 0.001%]	$5.6878.10^{-04}$ [0.2%]	$5.7057.10^{-04}$ [0.02%]
4	1	$1.8841.10^{-11}$	$1.8803.10^{-11}$ [0.2%]	$1.8692.10^{-11}$ [0.8%]	$1.8825.10^{-11}$ [0.09%]
4	2	$5.6213.10^{-08}$	$5.6195.10^{-08}$ [0.03%]	$5.5926.10^{-08}$ [0.5%]	$5.6215.10^{-08}$ [0.003%]
4	3	$1.2934.10^{-06}$	$1.2934.10^{-06}$ [0.003%]	$1.2933.10^{-06}$ [0.01%]	$1.2937.10^{-06}$ [0.02%]
4	4	$1.0583.10^{-04}$	$1.0584.10^{-04}$ [0.01%]	$1.0518.10^{-04}$ [0.6%]	$1.0586.10^{-04}$ [0.03%]
5	1	$2.8293.10^{-14}$	$2.8206.10^{-14}$ [0.3%]	$2.8090.10^{-14}$ [0.7%]	$2.8237.10^{-14}$ [0.2%]
5	2	$6.2509.10^{-11}$	$6.2479.10^{-11}$ [0.05%]	$6.1679.10^{-11}$ [1.3%]	$6.2509.10^{-11}$ [0.001%]
5	3	$2.4487.10^{-08}$	$2.4486.10^{-08}$ [0.002%]	$2.4227.10^{-08}$ [1.1%]	$2.4494.10^{-08}$ [0.03%]
5	4	$2.7598.10^{-07}$	$2.7603.10^{-07}$ [0.02%]	$2.7114.10^{-07}$ [1.8%]	$2.7613.10^{-07}$ [0.05%]
5	5	$2.1175.10^{-05}$	$2.1179.10^{-05}$ [0.02%]	$2.0933.10^{-05}$ [1.2%]	$2.1190.10^{-05}$ [0.07%]
Total		$4.5449.10^{-03}$	$4.5446.10^{-03}$ [0.007%]	$4.5369.10^{-03}$ [0.2%]	$4.5452.10^{-03}$ [0.005%]

Table: Circular orbit: angular momentum flux $\dot{L}_{\ell m}$ values at infinity, for different ℓm modes and $\ell < 5$ (units of M/m_0^2). The semi-latus rectum is $p = 7.9456$. The first column lists our results, and the second those of Poisson (1995,1997), the third of Martel (2004), the fourth of Sopuerta and Laguna (2006).

Geodesic waveforms (2nd order): elliptic ($<\dot{E}^\infty>$, $<\dot{L}^\infty>$)

e	p	$<\dot{E}^\infty>$	$<\dot{E}^\infty>$ Cutler *et al.* (1994)	$<\dot{E}^\infty>$ Martel (2004)	$<\dot{E}^\infty>$ Sopuerta, Laguna (2006)
0.188917	7.50478	$3.1617.10^{-04}$	$3.1680.10^{-04}$[0.2%]	$3.1770.10^{-04}$[0.5%]	$3.1640.10^{-04}$[0.07%]
0.764124	8.75455	$2.1026.10^{-04}$	$2.1008.10^{-04}$[0.09%]	$2.1484.10^{-04}$[2.1%]	$2.1004.10^{-04}$[0.1%]

Table: Elliptic orbit: average of the energy flux (units of M^2/m_0^2), taken over a few periods in the case of two elliptic orbits (e,p)=$(0.188917, 7.50478)$ and $(0.764124, 8.75455)$. The differences with the results of Cutler *et al.* (1994), Martel (2004), and Sopuerta and Laguna (2006) are shown.

e	p	$<\dot{L}^\infty>$	$<\dot{L}^\infty>$ Cutler *et al.* (1994)	$<\dot{L}^\infty>$ Martel (2004)	$<\dot{L}^\infty>$ Sopuerta, Laguna (2006)
0.188917	7.50478	$5.9550.10^{-03}$	$5.9656.10^{-03}$[0.2%]	$5.9329.10^{-03}$[0.4%]	$5.9555.10^{-03}$[0.008%]
0.764124	8.75455	$2.7531.10^{-03}$	$2.7503.10^{-03}$[0.1%]	$2.7932.10^{-03}$[1.4%]	$2.7505.10^{-03}$[0.09%]

Table: Elliptic orbit: average of the angular momentum flux (units of M/m_0^2) taken over a few periods in the case of two elliptic orbits (e,p)=$(0.188917, 7.50478)$ and $(0.764124, 8.75455)$. The differences with the results of Cutler *et al.* (1994), Martel (2004), and Sopuerta and Laguna (2006) are shown.

ℓ	$< \dot{E}_\ell^\infty >$	$< \dot{E}_\ell^\infty >$ Hopper, Evans (2010)	$< \dot{L}_\ell^\infty >$	$< \dot{L}_\ell^\infty >$ Hopper, Evans (2010)
2	$1.571333.10^{-04}$	$1.57133846.10^{-04}$[0.0004%]	$2.092406.10^{-03}$	$2.09219582.10^{-03}$[0.01%]
3	$3.776283.10^{-05}$	$3.77696202.10^{-05}$[0.02%]	$4.745961.10^{-04}$	$4.74663748.10^{-04}$[0.01%]
4	$1.149375.10^{-05}$	$1.14987458.10^{-05}$[0.04%]	$1.399210.10^{-04}$	$1.39978027.10^{-04}$[0.04%]
5	$3.837470.10^{-06}$	$3.84046353.10^{-06}$[0.08%]	$4.575322.10^{-05}$	$4.57886526.10^{-05}$[0.08%]
Total	$2.102273.10^{-04}$	$2.10242676.10^{-04}$[0.007%]	$2.752676.10^{-03}$	$2.75262625.10^{-03}$[0.002%]

Table: Elliptic orbit: average of the ℓ-mode energy (units of M^2/m_0^2) and angular momentum (units of M/m_0^2) fluxes radiated to infinity and taken over a few periods in the case of an elliptic orbit (e, p)=$(0.764124, 8.75455)$. Each ℓ-mode is obtained by summing the flux over all the azimuthal m-modes such that $(\dot{E}_\ell^\infty, \dot{L}_\ell^\infty) = \sum_{m=-\ell}^{\ell} (\dot{E}_{\ell m}^\infty, \dot{L}_{\ell m}^\infty)$. The differences with the results of Hopper and Evans (2010) are shown.

p	E^∞	E^∞ Martel (2004)	E^∞ Sopuerta, Laguna (2006)	E^{eh}	E^{eh} Martel (2004)	E^{eh} Sopuerta, Laguna (2006)
8.00001	3.5820	3.6703[2.4%]	3.5603[0.6%]	$1.8900.10^{-1}$	$1.8876.10^{-1}$[0.1%]	$1.8884.10^{-1}$[0.008%]
8.001	2.2350	2.2809[2.0%]	2.2212[0.6%]	$1.1349.10^{-1}$	$1.1260.10^{-1}$[0.8%]	$1.1339.10^{-1}$[0.09%]

Table: Parabolic orbit: energy radiated to infinity E^∞, and to the horizon E^{eh} (units of M/m_0^2) for $p \simeq 8$. The differences with the results of Martel (2004), and Sopuerta and Laguna (2006) are shown.

p	L^∞	L^∞ Martel (2004)	L^∞ Sopuerta, Laguna (2006)	L^{eh}	L^{eh} Martel (2004)	L^{eh} Sopuerta, Laguna (2006)
8.00001	$2.9596.10^1$	$3.0133.10^1$[1.8%]	$2.9415.10^1$[0.6%]	1.5137	1.5208[0.5%]	1.5112[0.2%]
8.001	$1.8813.10^1$	$1.9088.10^1$[1.4%]	$1.8704.10^1$[0.6%]	$9.0964.10^{-1}$	$9.1166.10^{-1}$[0.2%]	$9.0783.10^{-1}$[0.2%]

Table: Parabolic orbit: angular momentum radiated to infinity L^∞, and to the horizon L^{eh} (units of $1/m_0^2$) for $p \simeq 8$. The differences with the results of Martel (2004), and Sopuerta and Laguna (2006) are shown.

First order perturbation equation

Geodesic motion in the backgrouns metric

$$\frac{D^2 z^\alpha}{d\tau^2} = \frac{d^2 z^\alpha}{d\tau^2} + {}^b\Gamma^\alpha_{\mu\nu} u^\mu u^\nu = \frac{d^2 z^\alpha}{d\tau^2} + {}^b\Gamma^\alpha_{\mu\nu} \frac{dz^\mu}{d\tau}\frac{dz^\nu}{d\tau} = 0 \tag{14}$$

Through the Dirac-Detweiler-Whiting radiative perturbation, it is possible to suppose that the particle crosses the perturbed spacetime under geodesic motion

$$\frac{D^2 \hat{z}^\alpha}{d\lambda^2} = \frac{d^2 \hat{z}^\alpha}{d\lambda^2} + {}^f\Gamma^\alpha_{\mu\nu} \hat{u}^\mu \hat{u}^\nu = \frac{d^2 \hat{z}^\alpha}{d\lambda^2} + {}^f\Gamma^\alpha_{\mu\nu} \frac{d\hat{z}^\mu}{d\lambda}\frac{d\hat{z}^\nu}{d\lambda} = 0 \tag{15}$$

τ and λ: proper time in the -b- and -f- metric, respectively.
$\hat{z}^\alpha = z_g^\alpha + \Delta z^\alpha$: coordinates of m in $g_{\mu\nu} + h^*_{\mu\nu}$, where $h^*_{\mu\nu}$ is the DeWh radiative (effective) or the MiSaTuQuWa tail perturbation.

Computing the difference between these two geodesics, we get
Spallicci, Ritter, Aoudia (IJGMMP 2014)

$$\frac{D^2 \Delta z^\alpha}{d\tau^2} = \underbrace{-R_{\mu\beta\nu}{}^\alpha u^\mu \Delta z^\beta u^\nu}_{\text{Background geodesic deviation}} \quad \underbrace{-\frac{1}{2}(g^{\alpha\beta} + u^\alpha u^\beta)(2h^*_{\mu\beta;\nu} - h^*_{\mu\nu;\beta})u^\mu u^\nu}_{\text{Self-acceleration MiSaTaQuWa-DeWh}} \quad . \tag{16}$$

The BGD term is an out-product of the SF.

Self-force on radial fall. Why? hardly any time for cumulation

1. Plunges and highly eccentric orbits (EMR bursts) much more frequent than expected for non-rotating BHs (Amaro-Seoane, Sopuerta).
2. Jets and tidal disruption (Mashhoon et al.)
3. Plunges differ if non-SD black hole, like boson stars, or reveal dark matter (Kesden et al., Macedo et al.).
4. In particle physics, transplanckian regime and black hole production, back-action has a pivotal role in head-on collisions (Gal'tsov et al.).
5. Application and verification of the indirect method.
6. Comparison with NR (now only head-on collisions for large mass ratio).
7. Lousto (2000) self-force is repulsive, divergence at the horizon, ℓ dependency while Barack, Lousto (2001) self-force is attractive *but without analysis of the impact on the trajectory*.
8. de Donder (harmonic) and Regge-Wheeler gauges: regular transformation (for radial only). The mode-sum regularisation is carried out entirely in RW gauge.
9. The most non-adiabatic orbit of all. Full justification for self-consistency.
10. Does a self-consistent computation bring any difference?
11. Worthwhile problem à la Feynman: *I do it because I can solve it*.
12. Epistemology: it measures knowledge in physics (stone, tower, apple, lift, EMRI).
13. The most classic problem in gravitation ever.

Self-force: the pragmatic approach

- Pragmatic approach computes the correction in t and not τ time.

$$\Delta\ddot{r} = \underbrace{\Lambda_0\left(g, \dot{r}_g\right)\Delta r + \Lambda_1\left(g, \dot{r}_g\right)\Delta\dot{r}}_{\text{Background geodesic deviation}} \quad + \quad \underbrace{\Lambda_2\left(h, \dot{r}_g\right)}_{\text{Self acceleration}}$$

$$\Lambda_0 = -\frac{M}{r^2}\left[\frac{6M}{r^2} - \frac{2}{r} + \frac{6(r-M)}{r^2}\left(1-\frac{2M}{r}\right)^{-2}\dot{z}_g^2\right]\Delta z \qquad \Lambda_1 = \frac{6M}{r^2}\left(1-\frac{2M}{r}\right)^{-1}\dot{z}_g\Delta\dot{z} \qquad (17)$$

$$\Lambda_2 = \frac{1}{r-2M}\left[\frac{r^2 H_{0,t}}{2(r-2M)} - \frac{MH_1}{r-2M} - rH_{1,r}\right]\dot{z}_g^3 - \frac{3}{2}H_{0,r}\dot{z}_g^2 - 3\left(\frac{H_{0,t}}{2} - \frac{MH_1}{r^2}\right)\dot{z}_g + \frac{r-2M}{r}\left[\frac{2MH_0}{r^2} + \frac{(r-2M)H_{0,r}}{2r} - H_{1,t}\right]$$

Features include:

- Numerical computation of first order derivatives of the perturbations (third order derivatives of the wave function). It implies a fourth order scheme.

Fourth order stencil

Ten points are need. Eight possible ways to cross the stencil.

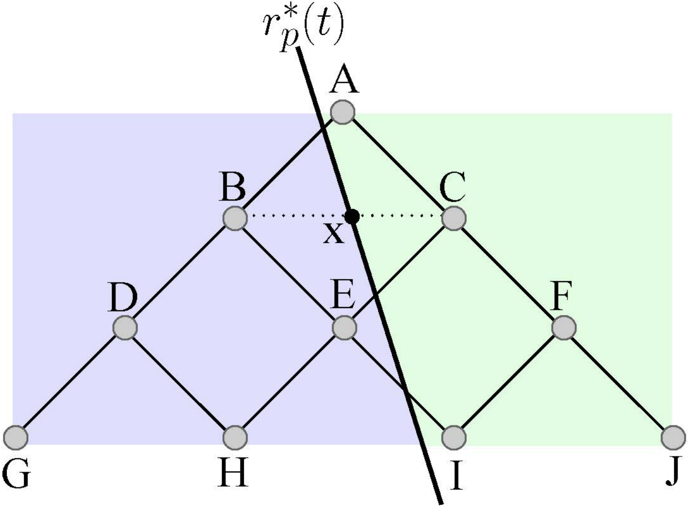

Pragmatic results

Table: The four zones according to the sign of Δr, $\Delta \dot{r}$, $\Delta \ddot{r}$.

Zone	IV $r_g - 1.2\ r_g$	III $1.2\ r_g - 2.2\ r_g$	II $2.2\ r_g - 3.5\ r_g$	I $3.5\ r_g - r_0$
Δr	-	-	-	-
$\Delta \dot{r}$	$+$	$+$	-	-
$\Delta \ddot{r}$	-	$+$	$+$	-

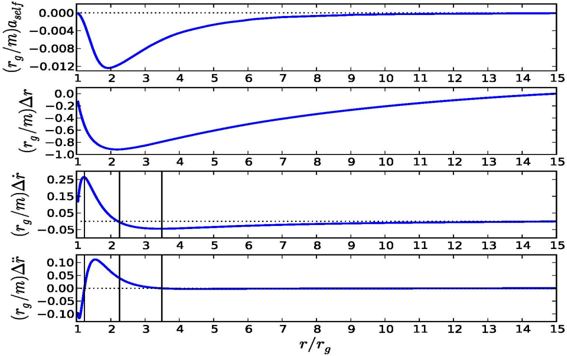

Pragmatic results: black hole premises reached earlier

- Zone I, particle falls faster than geodesic.
- Zone II, acceleration deviation turns positive, velocity deviation remains negative.
- Zone III, breaking is stronger and also velocity deviation turns positive.
- Zone IV, acceleration deviation reappears negative, but velocity deviation remains positive.
- At horizon, all deviation quantities approach zero, and agree with classic stand point.
- The self-quantities act always inward the black hole. Conversely, the geodesic deviation is repulsive (except the acceleration close to the horizon), and often of larger magnitude than self-quantities. Incidentally, $a_1 \Delta r$ and $a_2 \Delta \dot{r}$ have opposite signs.
- The maximal coordinate velocity $|dr/dt|_{\max}$ is not any longer $0.3592c$ but increases of $5m/M\%$, while $r_{\max} = 2.647 r_{\rm g}$ moves towards larger r.
- The back-action is dominated by the $l = 2$ mode, about 55% of the total.
- Uniform behaviour of $a_{\rm ret}$ and $a_{\rm self}$ *vis à vis* the different ℓ modes
- For increasing r_0, Δr increases (like $\Delta \dot{r}$).

Zone	IV	III	II	I
	$r_{\rm g} - 1.2\ r_{\rm g}$	$1.2\ r_{\rm g} - 2.2\ r_{\rm g}$	$2.2\ r_{\rm g} - 3.5\ r_{\rm g}$	$3.5\ r_{\rm g} - r_0$
Δr	-	-	-	-
$\Delta \dot{r}$	$+$	$+$	-	-
$\Delta \ddot{r}$	-	$+$	$+$	-

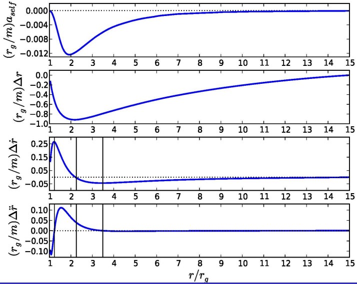

Pragmatic results

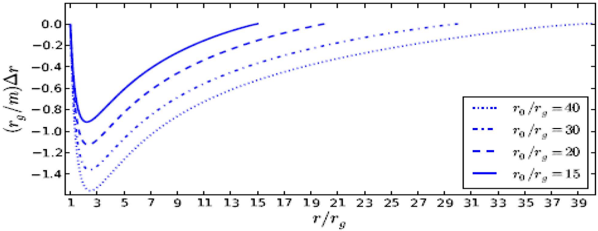

Self-consistent

- At late times Δr grows considerably.
- The self-consistent prescription describes motion continuously corrected.
  $e^x|_0 \sim 1 + x + \frac{x^2}{2}$ replaced by
  $e^x|_0 \sim 1 \rightarrow e^x|_1 \sim e + e(x-1) \rightarrow e^x|_2 \sim e^2 + e^2(x-2)$ *et caetera*.
- Gralla-Wald prescription: At each successive instant, the geodesic is corrected by the self-acceleration and a new geodesic is determined (without BGD). In a numerical implementation, the corrections will occur at discrete steps between short stretches of geodesics (BGD included).
- The equations of motion at n$^{\text{th}}$ order perturbation theory are more accurate than the (n-1)$^{\text{th}}$ equations, but at late times the corrections at n$^{\text{th}}$ order will become comparable to the corrections at (n-1)$^{\text{th}}$ order.
- The self-consistent approach can be applied at first order, as well as at higher orders. There isn't a conceptual impediment.
- Two ways to implement self-consistency: through stretches of osculating geodesics (the case here), or computing self-force quantities and mode-sum parameters on the 'real' non-geodesic trajectory (never done for a gravitational case).

Evolution: self-consistent prescription. II

$$
\begin{cases}
\nabla^\gamma \nabla_\gamma \tilde{h}_{\alpha\beta} - 2R^\gamma{}_{\alpha\beta}{}^\delta \tilde{h}_{\gamma\delta} = -16\pi m u_\alpha(t) u_\beta(t) \dfrac{\delta^{(3)}\left[x^\mu - z_p^\mu(t)\right]}{\sqrt{-g}} \dfrac{d\tau}{dt} \\
u^\beta \nabla_\beta u^\alpha = -(g^{\alpha\beta} + u^\alpha u^\beta)(\nabla_\delta h^{\rm tail}_{\beta\gamma} - \dfrac{1}{2}\nabla_\beta h^{\rm tail}_{\gamma\delta}) u^\gamma u^\delta \\
h^{\rm tail}_{\alpha\beta}(x) = m \displaystyle\int_{-\infty}^{\tau^-_{\rm ret}} \left(G^+_{\alpha\beta\alpha'\beta'} - \frac{1}{2} g_{\alpha\beta} G^{+\gamma}_{\gamma\alpha'\beta'} \right) \left[x, z_p(\tau')\right] u^{\alpha'} u^{\beta'} d\tau'
\end{cases}
\tag{18}
$$

where $u^\alpha(\tau)$, normalised in the background metric, refers to the self-consistent motion $z_p(\tau)$; $G^+_{\alpha\beta\alpha'\beta'}$ is the retarded Green function; the symbol $\tau^-_{\rm ret}$ indicates the range of the integral being extended just short of the retarded time $\tau_{\rm ret}$, so that only the interior part of the light-cone is used; note the use of $h^{\rm tail}_{\beta\gamma}$ equivalent to $h^R_{\beta\gamma}$ for our purposes. Difficulties include:

- System of 3 eqs. for each of the 10 metric components (harmonic gauge $\Rightarrow \nexists$ wave equation). At each integration step:
- 30 eqs. have to be computed for an adequate number of modes (work in spherical harmonics).
- Regularisation by mode-sum (or Riemann-Hurwitz ζ).
- Geodesic correction, crossed cell identification, source term computation.

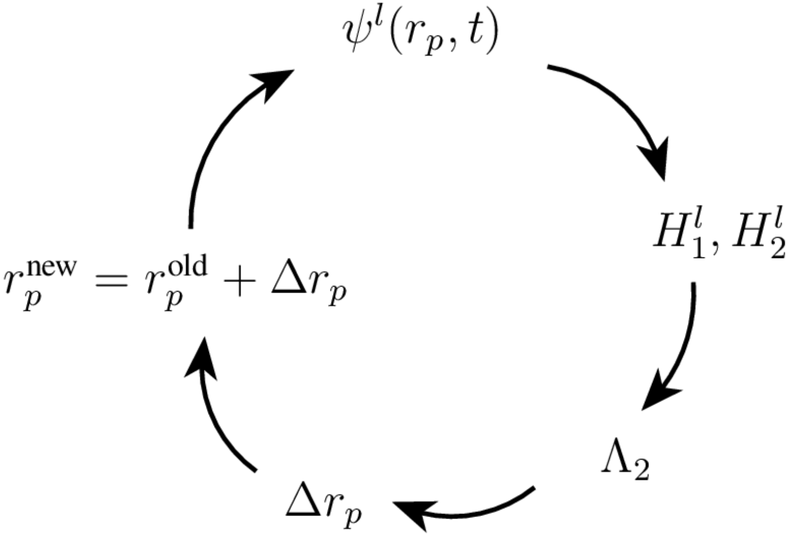
$\psi^l(r_p, t)$
H_1^l, H_2^l
Λ_2
Δr_p
$r_p^{\mathrm{new}} = r_p^{\mathrm{old}} + \Delta r_p$

Evolution: the iterative correction at work. II

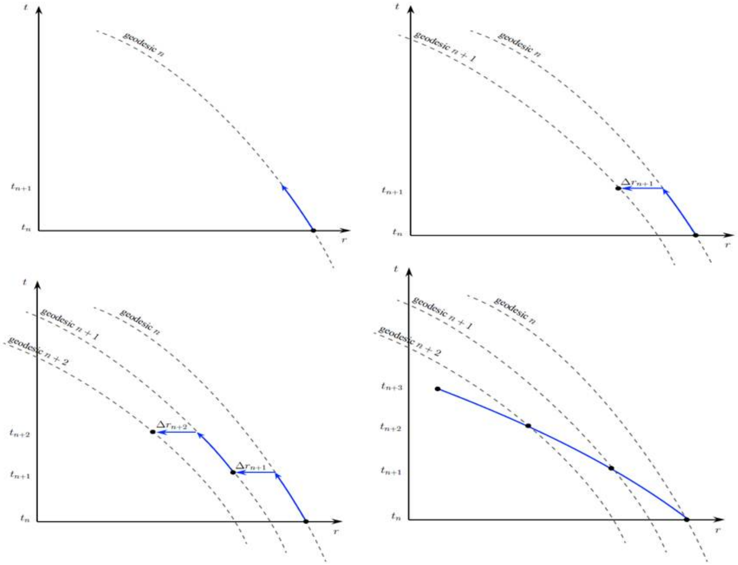

Pragmatic versus self-consistent (osculating)

$a_{\rm self}$, Δr, $\Delta \dot{r}$, and $\Delta \ddot{r}$ from the pragmatic and self-consistent (osculating) methods, and their difference, for $r_0 = 15 r_g$. The amplitudes, when computed self-consistently, differ of about 3% after $4 r_g$, and the four zones are slightly shifted towards the horizon.

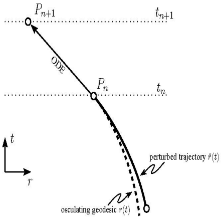

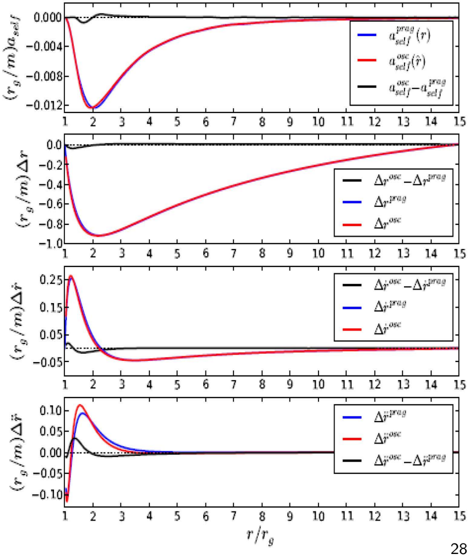

Production on low frequency sources

- Pierro V., Pinto I., Spallicci A., Laserra A., Recano F., 2001. *Fast and accurate computational tools for gravitational waveforms from binary systems with any orbital eccentricity*, Mon. Not. Roy. Astr. Soc., 325, 358, arXiv:gr-qc/0005044.
- Pierro V., Pinto I., Spallicci A., 2002. *Computation of hyperngeometric functions for gravitationally radiating binary stars*, Mon. Not. Roy. Astr. Soc., 334, 855.
- **Spallicci A. Aoudia S., 2004.** *Perturbation method in the assessment of radiation reaction in the capture of stars by black holes*, **Class. Q. Grav., 21, S563, arXiv:gr-qc/0309039.**
- Chauvineau B., Spallicci A., Fournier J.-D., 2005. *Brans-Dicke gravity in the capture of stars by black holes: some asymptotic results*, Class. Q. Grav., 22, S457, arXiv:gr-qc/0412053.
- **Aoudia S., Spallicci A., 2011.** *A source-free integration method for black hole perturbations and self-force computation: Radial fall*, **Phys. Rev. D, 83, 064029, arXiv:1008.2507 [gr-qc].**
- Blanchet L., Spallicci A., Whiting B., 2011. *Mass and motion in general relativity*, Springer Series on Fundamental Theory of Physics.
- **Ritter P., Spallicci A., Aoudia S., Cordier S., 2011.** *Fourth order indirect integration method for black hole perturbations: even modes*, **Class. Q. Grav., 28, 134012, arXiv:1102.2404 [gr-qc].**
- Spallicci A., 2013. *On the complementarity of pulsar timing and space laser interferometry for the individual detection of supermassive black hole binaries*, Astrophys. J., 764, 187, arXiv:1107.5984 [gr-qc].
- **Spallicci A., Ritter P., Aoudia S., 2014.** *Self-force driven motion in curved spacetime*, **to appear in Int. J. Geom. Meth. Mod. Phys., arXiv:1405.4155 [gr-qc].**
- **Spallicci A., Ritter P., 2014.** *A fully relativistic radial fall*, **submitted.**
- **Ritter P., Spallicci A., Aoudia S., Cordier S., 2014.** *Indirect (source-free) integration method for EMRIs: geodesic generic orbits and self-force consistent radial fall*, **in preparation.**

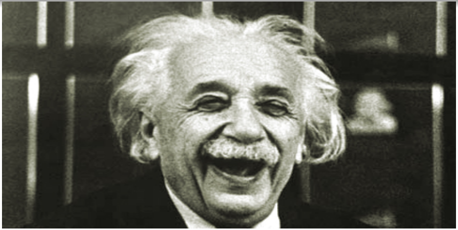

How does it happen that a properly endowed natural scientist comes to concern himself with epistemology?
Is there not some more valuable work to be done in his specialty? That's what I hear many of my colleagues ask, and I sense it from many more. But I cannot share this sentiment. When I think about the ablest students whom I have encountered in my teaching - that is, those who distinguish themselves by their independence of judgment and not just their quick-wittedness - I can affirm that they had a vigorous interest in epistemology. They happily began discussions about the goals and methods of science, and they showed unequivocally, through tenacious defense of their views, that the subject seemed important to them.